ISSN impresa 0717-3644
ISSN online 0718-221X

Maderas. Ciencia y tecnología 2021 (23): 65, 1-12

DOI: 10.4067/s0718-221x2021000100465

AUTOMATIC IDENTIFICATION OF CHARCOAL ORIGIN BASED ON DEEP LEARNING

***Ricardo Rodrigues de Oliveira Neto*[1,♠]**

***Larissa Ferreira Rodrigues*[2]**

***João Fernando Mari*[2]**

***Murilo Coelho Naldi*[3]**

***Emerson Gomes Milagres*[1]**

***Benedito Rocha Vital*[1]**

***Angélica de Cássia Oliveira Carneiro*[1]**

***Daniel Henrique Breda Binoti*[4]**

***Pablo Falco Lopes*[4]**

***Helio Garcia Leite*[1]**

ABSTRACT

The differentiation between the charcoal produced from (*Eucalyptus*) plantations and native forests is essential to control, commercialization, and supervision of its production in Brazil. The main contribution of this study is to identify the charcoal origin using macroscopic images and Deep Learning Algorithm. We applied a Convolutional Neural Network (CNN) using VGG-16 architecture, with preprocessing based on contrast enhancement and data augmentation with rotation over the training set images. on the performance of the CNN with fine-tuning using 360 macroscopic charcoal images from the plantation and native forests. The results pointed out that our method provides new perspectives to identify the charcoal origin, achieving results upper 95 % of mean accuracy to classify charcoal from native forests for all compared preprocessing strategies.

Keywords: Charcoal, classification, deep learning, native wood, preprocessing.

INTRODUCTION

Brazil is one of the largest charcoal producers, with a reaching 5,3 million tons in 2019 (Ministry of Mines and Energy 2020). Besides being a world producer, Brazil is also one of the largest consumers of charcoal. Most of this production is destined for the internal market, mainly for the pig-iron and steel sectors and lesser, for the ferroalloy sector and residential consumption (ABRAF 2013). However, this demand is not supplied through charcoal using planted forests, making the illegal exploitation of native forests attractive.

In order to try to prevent this illegal production, the Ministry of the Environment, through Ordinance No. 253/2006, established the Forest Origin Document (DOF), an obligatory license for the transportation and

[1]Federal University of Viçosa, Department of Forest Engineering, Viçosa, MG, Brazil.
[2]Federal University of Viçosa, Institute of Exact and Technological Sciences, Rio Paranaíba, MG, Brazil.
[3]Federal University of São Carlos, Department of Computer Science, São Carlos, SP, Brazil.
[4]DAP Florestal, Centro Empresarial da Serra. Parque Res. de Laranjeiras, Serra, ES, Brazil.
[♠]Corresponding author: ricardo.rodrigues@ufv.br
Received: 20.02.2020 Accepted: 04.08.2021

storage of forest products and by-products, that includes information about the origin of those products. This li-cense expired in cases when the transported product does not correspond to the species authorized in the DOF. In this context, forensic identification is used in the analysis of the preserved wood in charcoal to determine his origin (Gonçalves *et al.* 2012, Nisgoski *et al.* 2014), i.e., to distinguish those produced with native forests from those from planted forests, mainly composed of species of *Eucalyptus* (Davrieux *et al.* 2010). The principal clones used to produce charcoal are *Eucalyptus urophylla*, *E. grandis*, and hybrids *E. urophylla x grandis*, *E. urophylla x camaldulensis*, and *E. grandis x camaldulensis* (Santos 2010, Pereira *et al.* 2012).

Usually, the anatomic analysis of charcoal can be done through a macro or microscopic approach. In the microscopic identification is observed features of the tissues and the constituent cells of the wood (Zenid and Ceccantini 2012), while in macroscopic analysis, only anatomical features visible to the naked eye or with a magnifying glass, such as vessel arrangement and grouping, arrangement and abundance of axial parenchyma and ray width (Wheeler and Baas 1998). Both analyses can be used in the distinction between *Eucalyptus* and other genera.

Much has been proposed on the microscopic analysis, as reported in the studies proposed by Gonçalves *et al.* 2012, Albuquerque (2012) and Muñiz *et al.* (2012), with higher cost and limited logistics, can identify the charcoal to the level of species with trustable results, although this is not always necessary for charcoal iden-tification for supervision purpose. On the other hand, just a few studies have been proposed the macroscopic analysis to distinguish the origin of charcoal, although it allows agility and practicality. The genus *Eucalyptus* present a homogeneous anatomical constitution among the species, under the morphological level, a factor that hinders the separation, based only on the composition and structural arrangement of the wood constituents (Tomazello-Filho 1985, Oliveira 1997). This similarity can help in distinguishing this genus from the others.

Digital image process and machine learning techniques are essential to this task because it allows the acquisition of visual features for the automatic classification. Some studies proposed to classify charcoal images with a non-automated user-based process. Khalid *et al.* (2008) proposed a method based on analysis of anatomical images of the transverse plane in order to differentiate charcoals of the genus *Eucalyptus* sp. from charcoal of native species. Andrade *et al.* (2019) proposed a system of classification of the origin of the char-coal using analysis of texture in digital images of the cross-section plane. For this, a database was produced containing 900 images of 18 species, 12 native and 6 of the genus *Eucalyptus* sp. After, texture features were extracted from each image using Level Co-occurrence Matrices (GLCM) (Haralick *et al.* 1973), which were used in training and in the evaluation of statistical classifiers that identified the origin of the charcoals correctly in about 97 % of the attempts.

However, the previously cited works do not add much to the identification of the origin of the charcoal in the field, due to the subjective, expensive logistic limitation imposed by the use of microscopes and the preparation of the material. The computational resources advances have allowed deep learning approach out-performs techniques based on handcrafted feature extraction on several fields such as computer-aided medical diagnosis systems (Litjens *et al.* 2017, Rodrigues *et al.* 2020), remote sensing (Nogueira *et al.* 2017, Zhu *et al.* 2017), forest species recognition (Hafemann *et al.* 2014), identification of ecosystems (Morales *et al.* 2018, Bayr and Puschmann 2019), agriculture (Kamilaris and Prenafeta-Boldú 2018, Knoll *et al.* 2018), and other applications (Gu *et al.* 2018).

Recently, Maruyama *et al.* (2018) proposed a method for automatic classification of native species of charcoal based on deep learning using Inception-V3 architecture (Szegedy *et al.* 2016) as a feature extractor. However, it was considered microscopy images, and these experiments performed a simple holdout validation technique (Devijver and Kittler 1982), which can randomly create biased sets, causing the CNNs to fit non-rep-resentative (abnormal) samples and result in unexpected accuracies. Differently, we considered the VGG-16 architecture (Simonyan and Zisserman 2014) instead of Inception-V3. The VGG-16 network was chosen due to its simplicity and robustness. Moreover, it was the first architecture to replace the filters that require more computational power, by large sequences of convolutional filters with size 3x3.

In this work, we study an efficient method for automatic identification of charcoal origin based on deep learning and cross-validation k-fold technique using macroscopic images. This is the first work to classify au-tomatically in order to distinguish *Eucalyptus* and native species using the VGG-16 architecture. Also, prepro-cessing strategies based on contrast enhancement, data centralization, and data augmentation on the rotation of the training set images were tested to increase the performance of the CNN with fine-tuning.

MATERIAL AND METHODS

The experiment was performed on a machine with an Intel i5 3,00 GHz processor, 16 GB RAM, and a GPU NVIDIA GeForce GTX 1050Ti with 4 GB memory. All experiments were programmed using Python 3.6, the PyTorch 1.7 deep learning framework (Paske *et al.* 2019) under CUDA version 10.1 (2019) and cuDNN 7.6 (2020). The operating system was Ubuntu 18.04.5 LTS.

Images acquisition

The dataset of macroscopic images of charcoal was acquired from Wood Panel and Energy Laboratory (LAPEM) at the Federal University of Viçosa (UFV), Brazil. The material is composed of samples of car-bonized wood of *Eucalyptus* and native species typical of the region of Zona da Mata, Minas Gerais. Native species were chosen based on the anatomical similarity to the genus *Eucalyptus* as well as their attractiveness to the illegal production of charcoal. *Eucalyptus* species were chosen from those predominantly used for the production of charcoal, as Pereira *et al.* (2012) define.

In this dataset, each species or hybrid is represented by a sample coming from a single tree, without infor-mation of age or position of the trunk. The samples were charred in a muffle-type electric furnace, following an initial temperature of 150 ºC, with an increase of 50 ºC per hour, and the final temperature of 450 ºC, totaling 7 hours of carbonization. The condensable gases were collected in a condenser coupled to the muffle door. The species and hybrids used in this study and the numbers of samples for each species are presented in Table 1.

Table 1: Species and hybrids used.

Identification	Common name	Scientific Name	Number of Samples
1	5 Folhas	*Sparattosperma leucanthum*	2
2	Açoita Cavalo	*Luehea divaricata*	7
3	Adraga	*Bixa orellana*	9
4	Algaroba	*Prosopis juliflora*	1
5	Angá	*Inga edulis*	2
6	Angico	*Anadenanthera peregrina* Speg	12
7	Barbatimão	*Stryphnodendron adstringens*	6
8	Bico de Pato	*Machaerium nyctitans*	9
9	Brauninha	*Dictyoloma vandellianum* A. Juss	8
10	Caituá	*Ouratea polygyna* Engl	1
11	Camaudulensis	*Eucalyptus camaldulensis* Dehnh	31
12	Citriodora	*Corymbia citriodora*	13
13	Canudo de Pito	*Mabea fistulifera*	17
14	Casca Doce	*Glycoxylon inophyllum*	2
15	Casuarina	*Casuarina equisetifolia* L.	6
16	Catingueira	*Caesalpinia pyramidalis*	1
17	Caviuna	*Machaerium scleroxylon*	2
18	Cedrinho	*Trattinninkia ferruginea* Kuhlm	10
19	Embaúba	*Cecropia pachystachya*	15
20	Fedegoso	*Senna macranthera*	5
21	Garapa	*Apuleia leiocarpa*	9
22	Grandis x Camaudulensis	*Eucalyptus grandis x Eucalyptus camaldulensis*	9
23	Imburana	*Commiphora leptophloeos*	3
24	Jacarandá da Bahia	*Dalbergia nigra*	2
25	Jambo	*Syzygium jambos*	4
26	Jurema Branca	*Mimosa tenuiflora*	3
27	Jurema Preta	*Mimosa hostillis*	2
28	Mama de Porca	*Zanthoxylum rhoifolium* Lam	4
29	Marmeleiro	*Cydonia oblonga* Mill	4
30	Mofumbo	*Combretum leprosum*	1
31	Papagaio	*Aegiphila integrifolia*	11
32	Pau Bosta	*Sclerolobium paniculatum*	5
33	Pau Fumo	*Piptocarpha macropoda* Baker	14
34	Pimenteira	*Xylopia sericea* A. St - Hil	8
35	Quina	*Bathysa sp*	13
36	Só Brasil	*Colubrina glandulosa*	18
37	Sucupira	*Pterodon emarginatus* Vogel	9
38	Urocam	*Eucalytus urophyla x Eucalyptus camaldulensis*	25
39	Urograndis	*Eucalyptus urophyla x Eucalyptus grandis*	31
40	Urophylla	*Eucalyptus urophyla* S. T. Blake	26

The images were acquired using equipment with led light illumination and support for a cell phone, generating images with 12 megapixels and optical zoom of 20 times. As the charcoal pieces were broken, and not cut, there was a large amount of non-flat surfaces. With this zoom, a larger area in which there are no irregular breaks on the surface of the charcoal (that made it difficult to analyze the distribution of cellular components) could be analyzed.

The dataset is composed of 360 charcoal images, in which 135 images are of *Eucalyptus* species, and 225 images of native species. An expert in wood anatomy analyzed the charcoal images classified them as *Eucalyptus* and native. To illustrate them, Table 2 shows information about name, quantity, and one image from each class. All images of charcoal dataset were categorized into two classes properly labeled: eucalyptus (135 images), and native (225 images). After, all images of the charcoal data set were randomly sampled and partitioned into five stratified sets (folds).

Table 2: Information about each class in the dataset.

Class	Quantity
Eucalyptus	135
Native	225
Total	360

Image preprocessing

All images were resized to 224 x 224 pixels, size allowed for the input of the CNN architecture used in this work. Then was applied one of the preprocessing methods and used to train and test the VGG-16 architecture.

Figure 1 shows samples of charcoal images considering each preprocessing strategy evaluated. The original image from the dataset is defined as a strategy (a) (i.e., no preprocessing). In (b), there is an example of contrast stretching strategy.

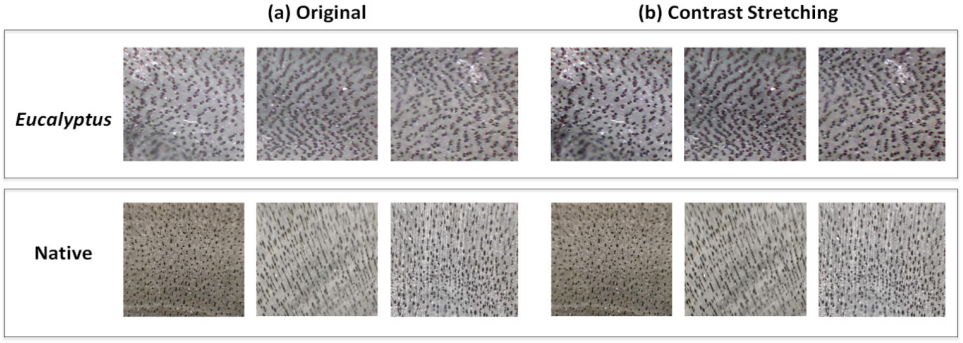

Figure 1: Contrast improvement applied in charcoal image: (a) original image (i.e. without preprocessing); (b) contrast stretching. Image instances from the charcoal dataset showing *Eucalyptus* (top) and native (bottom) classes.

Data augmentation

Data augmentation is a strategy that consists of increase the training data without increasing the number of samples (Krizhevsky *et al.* 2012). In this study, we applied data augmentation based on rotations of the images considering angles of between 0 º and 360 º with steps of 45 º, increasing the training set in 8 times.

Convolutional neural networks

The main concepts addressed in the Deep Learning paradigm were obtained from Neural Networks, which aims to develop computer programs capable of solving problems that are difficult to solve through formal rules (Goodfellow *et al.* 2016). The main characteristic of a Convolutional Neural Network (CNN) is to be com-posed mainly of convolutional layers, and its main application is the processing of visual information (Ponti *et al.* 2017). A CNN consists of three types of neural layers, described below (Guo *et al.* 2016).

Convolutional

The convolutional layer is generated through a set of filters over an input image. Each filter is responsible for detecting a specific type of feature. Figure 2 illustrates the basic structure of the convolutional layer define by C^l and composed by W_k^l filters with size of the spatial stent and the hyper-parameter from the input volume M^{l-1}. Finally, the convolution result is added to the bias *b*, generating K 2D feature maps stacked in an output volume M^l, defined by Equation 1 (Rodrigues *et al.* 2020).

$$M_k^l = \sum_{d=1}^{D} M_d^{l-1} W_d^l + b_k^l \quad (1)$$

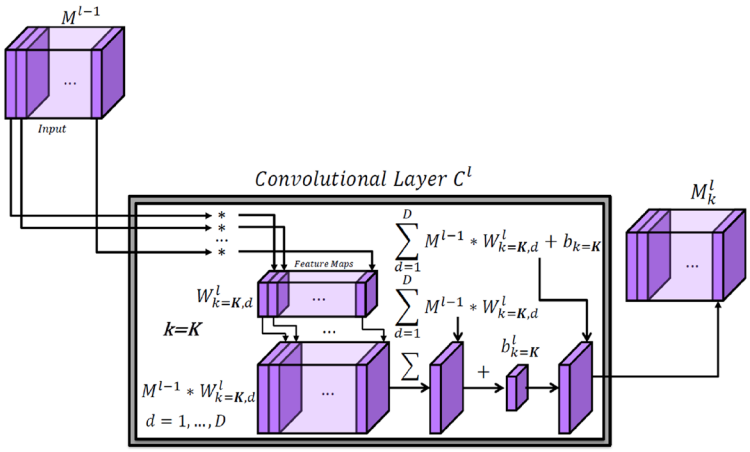

Figure 2: Illustration of the convolutional layer.

Pooling

The pooling layer allows reducing the size of feature maps considering maximum or average pooling. The CNN architecture considered in this paper applies maximum pooling because this criterion results in better generalization and faster convergence (Scherer *et al.* 2010). Figure 3 illustrates the maximum and average pooling considering a pooling layer with size 2 x 2.

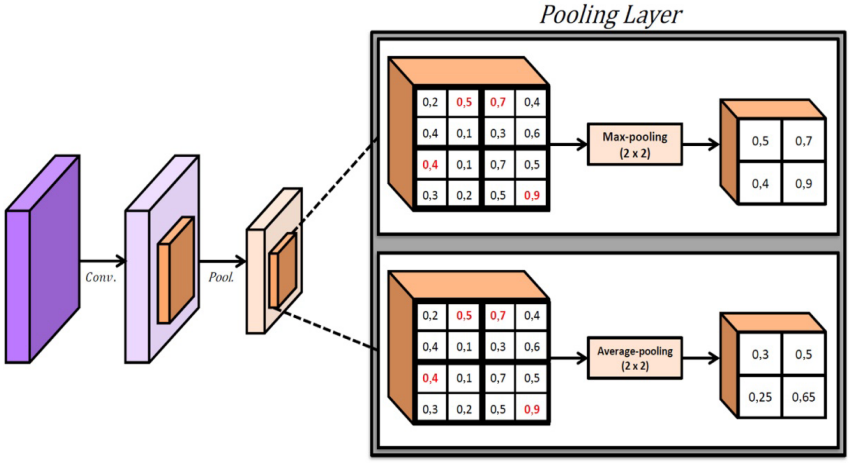

Figure 3: Illustration of the pooling layer and the computations to maximum and average pooling.

Fully connected

The fully connected layer is present in the last layers and converted the two-dimensional feature maps into a one-dimensional feature vector. Finally, the last layer is composed of softmax with neurons representing the number of classes in the dataset. Figure 4 illustrates the fully-connected layers after the convolutional and pooling layers and the softmax layer.

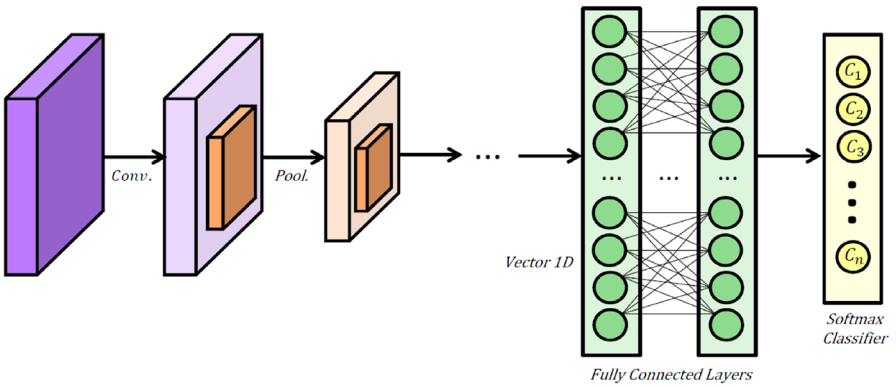

Figure 4: Illustration of the structure of fully-connected layers and softmax layer.

Training based on ine-tuning

The training strategy based on fine-tuning it is a practical and common approach for training deep learning architectures (Goodfellow *et al.* 2016). The network is previously trained for a classification task using a very large data set (Deng *et al*. 2009). The parameters values (weights) learned for the initial layers of the network are kept (frozen), and the top layers trained over the data set of interest, which are intended to learn the more complex structures of the data.

VGG-16 architecture

The VGG-16 network, which is composed of 13 convolutional layers, five pooling layers, and three fully-connected (considering the softmax)(Simonyan and Zisserman 2014), was chosen due to its simplicity and robustness. In this study, we evaluated the VGG-16 improved with batch normalization. This strategy maintains the mean output close to 0 and the output standard deviation close to 1, increasing stability across the network and leading to a faster learning rate (Ioffe and Szegedy 2015).

We keep fixed all convolutional layers blocks to maintain the parameters learned from training over the ImageNet dataset, while the top layers have their parameters adjusted using a small learning rate. Figure 5 illustrates the VGG-16, and the blue box indicates the fixed layers.

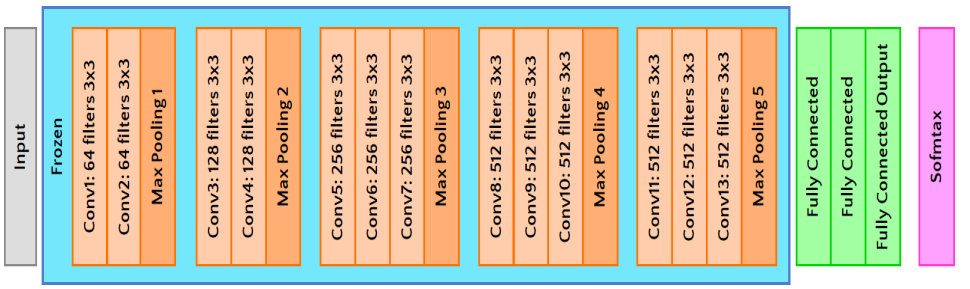

Figure 5: VGG-16 architecture. Blue box indicates the blocks of convolutional layers fixed during training based on fine-tuning.

The training of the VGG-16 is defined as an optimization problem to improve the quality of prediction. In this study, we considered the loss function as the objective function. The loss function used was binary cross-entropy function, commonly used for binary classification problems. In this way, we minimize this function using the Stochastic Gradient Descent (SGD) optimizer (Lecun *et al.* 1998), a popular optimization algorithm for parameter optimization of machine learning and deep learning models. It is based on a gradient descendent approximation using batches of randomly selected data samples instead of computing the gradient for each object of the dataset. Thus, the SGD optimizer allows finding iteratively the parameter values that minimize the loss function (cross-entropy) (Goodfellow *et al.* 2016).

VGG-16 was trained with a learning rate of 0,001, weight decay of $1e^{-6}$, a momentum of 0,9 momentum Nesterov, mini-batch size of 32, REctified Linear Unit (RELU) function, and training considering 100 epochs.

Validation

The validation of the classification is performed using k-fold cross-validation (Kohavi 1995) statistical method, which partition the data into k folds used for training and test. All images were sampled and parti-tioned into five stratified sets, i.e., the folds are build preserving (approximately) the proportion of examples for each class of the original set. We repeated the cross-validation five times, and for each iteration, one of the training folds is chosen for validation and the others for training.

Additionally, the mean value of accuracy (Equation 2) is used to quantify the quality of the results. The accuracy index is based on the number of true positives (TP), true negatives (TN), false positives (FP) and false negative (FN), computed from the confusion matrix, that allows verifying the number of correct classifications as opposed to the classifications predicted for each class (Duda *et al.* 2000).

$$Accuracy = \frac{TP + TN}{TP + TN + FP + FN} \qquad (2)$$

Also, to visualize the True Positive Rate (TPR) against the False Positive Rate (FPR) at various decision thresholds, it was considered the Receiver Operating Characteristic (ROC). The Area Under ROC (AUC) is used as a reliable classification performance measure of all possible classification thresholds (Fawcett 2006).

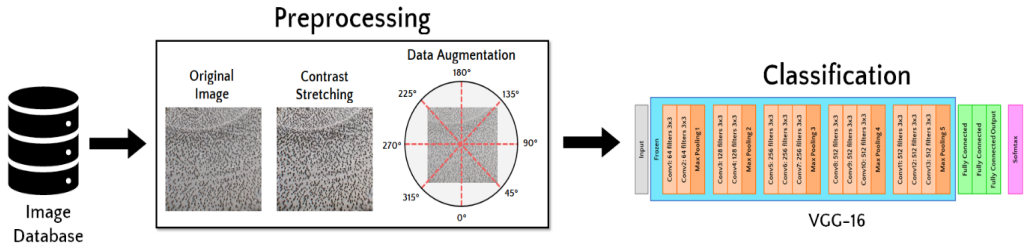

Figure 6: Approach proposed.

RESULTS AND DISCUSSION

We trained the VGG-16 architecture considering each contrast improvement strategy and average sub-traction. Figure 7 shows the evolution of the loss values and accuracy's for the considering the average of all k-fold iterations for each preprocessing strategy evaluated. This behavior result suggests that the training did not overfit the data and maintaining the generalization property of the CNN.

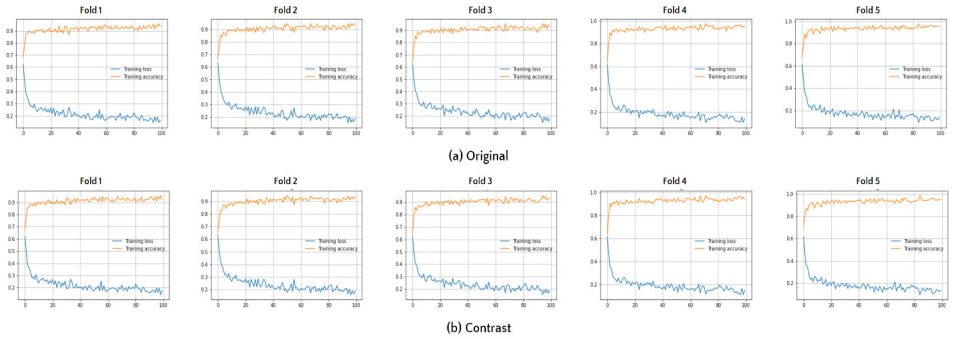

Figure 7: Evolution of accuracy values and loss values for each fold and each strategy evaluated

In order to assess the values of True Positive Rate (TPR) against the False Positive Rate (FPR) we analyzed the ROC (AUC) for each iteration of the k-fold. The evolution of these values is shown graphically in Figure 8. It is important to note that an AUC upper of 80% for most of the folds results in an average AUC of 84% and 81,6% for original and contrast stretching, respectively. Also, this result suggests that our approach is a promising method.

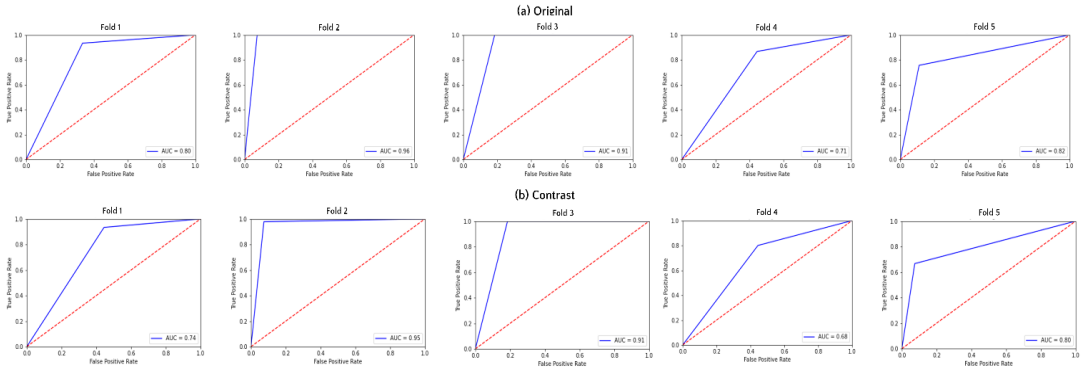

Figure 8: ROC curves for each fold.

The mean accuracy resulted from VGG-16 is presented in Table 3, considering each preprocessing strategy evaluated. The use of the original images is the best choice, resulting in a mean accuracy of 85,8%. The data centralization performed by average image subtraction has a positive impact, independently of preprocessing.

Table 3: Average test accuracy for each preprocessing strategy

Preprocessing Strategy	Accuracy (%)
Original	85,8
Contrast	83,0

The confusion matrices (Table 4) allow observing some aspect of the classification problem investigated in this work. The presented values were obtained for training with the whole training set and prediction over the validation set (which is the 3rd fold). It is worth noticing that the charcoal from native wood is rarely misclassified as eucalyptus, which is the main objective of this research, i.e., to provide a computational method capable of preventing the exploitation of native wood. Although the best overall result was obtained with the original images without preprocessing, it is possible to see that contrast widening allowed the identification of

97,78 % of native woods when fold-3 is considered.

Figure 9 shows samples of native images classified as *Eucalyptus* for each strategy tested. Although the goal is to perform a binary classification, we found that native species with few samples in the database such as *Cydonia oblonga* Mill, *Inga edulis*, *Prosopis juliflora*, and *Sclerolobium paniculatum* may be classified as *Eucalyptus*. Therefore, a small number of samples of these species results in a lack of visual patterns. Also, we observed that the other native species misclassified presents visual patterns similar to *Eucalyptus*, like an increase in the thickness and distribution of the vessels in the center - bark direction (de Jesus and Silva 2020).

Table 4: Confusion Matrix of the best result for each preprocessing strategy.

(a) Original				(b) Contrast		
	Eucalyptus	Native			*Eucalyptus*	Native
Eucalyptus	96,30	3,70		*Eucalyptus*	96,30	3,70
Native	4,44	95,56		Native	2,22	97,78

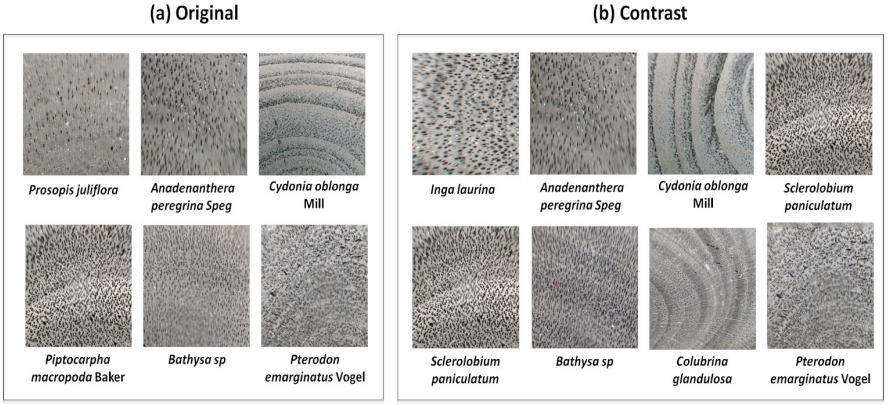

Figure 9: Examples of native images classified as *Eucalyptus* for each strategy evaluated.

CONCLUSIONS

The results allow concluding that, for the classification of charcoal images, the VGG-16 architecture obtained better results when the augmented data set is analyzed considering the average subtraction as preprocessing strategy (values lying on 85,8 %, in terms of accuracy). Also, after learning the particular features, the VGG-16 architecture resulted from the proposed method was able to classify charcoal from native forests, at least, 95 % mean accuracy using original images, i.e., without preprocessing strategy, and considering the 5-fold cross-validation procedure.

The presented results open new opportunities towards better exploiting deep learning for automatic classification between charcoal produced from planted wood (*Eucalyptus*), and those originated from native forests. As for future work, other data augmentation strategies may be tested, together with other normalization strategies and different types of convolutional neural networks.

ACKNOWLEDGMENTS

We gratefully acknowledge the support of NVIDIA Corporation, FAPEMIG for financial support, LAPEM (Panels and Wood Energy Laboratory) for the charcoal materials, and Institute of Exact and Technological Sciences (IEP UFV-CRP) for providing the resources for the acquisition of the GeForce GTX 1050Ti GPU used in this research. This study was financed in part by the Coordenação de Aperfeiçoamento de Pessoal de Nível Superior - Brasil (CAPES) - Finance Code 001.

REFERENCES

ABRAF. 2013. *ABRAF Statistical Yearbook 2013 - Base Year 2012*, Brasília, Brazil.

Albuquerque, Á.R. 2012. Anatomia comparada do lenho e do carvão aplicada na identificação de 76 espécies da floresta amazônica, no estado do Pará, Brasil. Master's Dissertation, University of São Paulo, Pi-racicaba, Brazil. https://dx.doi.org/10.11606/D.11.2012.tde-20092012-093146

Andrade, B.G.D.; Vital, B.R.; Carneiro, A.D.C.O.; Basso, V.M.; Pinto, F.D.A.D.C. 2019. Poten-tial of Texture Analysis for Charcoal Classification. *FLORAM* 26(3): 1-10. http://dx.doi.org/10.1590/2179-8087.124117

Bayr, U.; Puschmann, O. 2019. Automatic detection of woody vegetation in repeat landscape photographs using a convolutional neural network**.** *Ecol Inform* 50:220-233. https://doi.org/10.1016/j.ecoinf.2019.01.012

Davrieux, F.; Rousset, P.L.A.; Pastore, T.C.M.; Macedo, L.A. de; Quirino, W.F. 2010. Discrimination of native wood charcoal by infrared spectroscopy. *Quim Nova* 33(5): 1093-1097. http://dx.doi.org/10.1590/S0100-40422010000500016

Deng, J.; Dong, W.; Socher, R.; Li-Jia, L.; Fei-Fei, L. 2009. ImageNet: A large-scale hierarchical image database; In: IEEE Conference on Computer Vision and Pattern Recognition, Miami, FL, pp. 248-255. https://doi.org/10.1109/CVPR.2009.5206848

Devijver, P.A.; Kittler, J. 1982. *Pattern recognition: A statistical approach*. Prentice-Hall: London, UK.

Duda, R.O.; Hart, P.E.; Stork, D.G. 2000. *Pattern Classi ication (2nd Edition)*. New York, NY, USA: Wiley-Interscience.

Fawcett, T. 2006. An introduction to ROC analysis. *Pattern Recogn Lett* 27: 861-874. https://doi.org/10.1016/j.patrec.2005.10.010

Gonçalves, T.A.P.; Marcati, C.R.; Scheel-Ybert: R. 2012. The effect of carbonization on wood structure of *Dalbergia violacea*, *Stryphnodendron polyphyllum*, *Tapirira guianensis*, *Vochysia tucanorum*, and *Pouteria torta* from the brazilian cerrado. *Iawa J* 33(1): 73-90. https://doi.org/10.1163/22941932-90000081

Goodfellow, I.; Bengio, Y.; Courville, A. 2016. *Deep learning*. MIT Press: USA. http:/www.deeplearn-ingbook.org

Gu, J.; Wang, Z.; Kuen, J.; Ma, Lianyang.; Shahroudy, A.; Shuai, B.; Liu, T.; Wang, X.; Wang, L.; Wang, G.; Cai, J.; Chen, T. 2018. Recent advances in convolutional neural networks. *Pattern Recogn* 77: 354-377. https://doi.org/10.1016/j.patcog.2017.10.013

Guo, Y.; Liu, Y.; Oerlemans, A.; Lao, S.; Wu, S.; Lew, M.S. 2016. Deep learning for visual understand-ing: A review. *Neurocomputing* 187: 27-48. https://doi.org/10.1016/j.neucom.2015.09.116

Hafemann, L.G.; Oliveira, L.S.; Cavalin, P. 2014. Forest species recognition using deep convolutional neural networks. In: 2014 22nd International Conference on Pattern Recognition, Stockholm, Sweden, pp. 1103-1107. https://doi.org/10.1109/ICPR.2014.199

Haralick, R.M.; Shanmugam, K.; Dinstein, I. 1973. Textural features for image classification. *IEEE Transactions on Systems, Man, and Cybernetics* 6: 610-621. https://doi.org/10.1109/TSMC.1973.4309314

Ioffe, S.; Szegedy, C. 2015. Batch normalization: Accelerating deep network training by reducing internal covariate shift. Proceedings International conference on machine learning 37: 448-456. https://arxiv.org/pdf/1502.03167.pdf

de Jesus, D.S.; Silva, J.S. 2020. Variação radial de propriedades anatômicas e físicas da madeira de eucalipto. *Cadernos de Ciência & Tecnologia* 37(1): 26476. http://dx.doi.org/10.35977/0104-1096.cct2020. v37.26476

Kamilaris, A.; Prenafeta-Boldú, F.X. 2018. Deep learning in agriculture: A survey. *Comput and Electron in Agr* 147: 70-90. https://doi.org/10.1016/j.compag.2018.02.016

Khalid, M.; Lee, E.L.Y.; Yusof, R.; Nadaraj, M. 2008. Design of an intelligent wood species recognition system. *IJSSST* 9(3): 9-19. https://ijssst.info/Vol-09/No-3/paper2.pdf

Knoll, F.J.; Czymmek, V.; Poczihoski, S.; Holtorf, T.; Hussmann, S. 2018. Improving efficiency of organic farming by using a deep learning classification approach. *Comput Electron Agric* 153: 347-356. https://doi.org/10.1016/j.compag.2018.08.032

Kohavi, R. 1995. A study of cross-validation and bootstrap for accuracy estimation and model selection. In Proceedings of the 14th International Joint Conference on Artificial Intelligence - IJCAI'95, Volume 2: 1137-1143. Morgan Kaufmann Publishers Inc.: San Francisco, CA, USA.

Krizhevsky, A.; Sutskever, I.; Hinton, G.E. 2012. ImageNet classification with deep convolutional neu-ral networks. In Proceedings of the 25th International Conference on Neural Information Processing Systems - NIPS'12 Volume 1: 1097-1105. Curran Associates Inc.: Red Hook, NY, USA,

Lecun, Y.; Bottou, L.; Bengio, Y.; Haffner, P. 1998. Gradient-based learning applied to document recog-nition. Proceedings of the IEEE 86(11): 2278-2324. https://doi.org/10.1109/5.726791

Litjens, G.; Kooi, T.; Ehteshami-Bejnordi, B.; Setio, A.; Ciompi, F.; Ghafoorian, M.; van der Laak, J.; van Ginneken, B.; Sánchez**, C. 2017.** A survey on deep learning in medical image analysis. *Med Image Anal* 42: 60-88. https://doi.org/10.1016/j.media.2017.07.005

Maruyama, TM.; Oliveira, L.S.; Britto, A.S.; Nisgoski, S. 2018. Automatic classification of native wood charcoal. *Ecol Inform* 46: 1-7. https://doi.org/10.1016/j.ecoinf.2018.05.008

Ministry of Mines and Energy. 2020. Brazilian Energy Balance - year 2019. Ministry of Mines and Energy, Rio de Janeiro, Brazil. http://biblioteca.olade.org/opac-tmpl/Documentos/cg00828.pdf

Morales, G.; Kemper, G.; Sevillano, G.; Arteaga, D.; Ortega, I.; Telles, J. 2018. Automatic segmentation of *Mauritia flexuosa* in unmanned aerial vehicle (uav) imagery using deep learning. *Forests* 9(12):736. https://doi.org/10.3390/f9120736

Muñiz, G.I.B.; Nisgoski, S.; Shardosin, F.Z.; França, R.F. 2012. Anatomia do carvão de espécies florestais. *Cerne* 18(3): 471-477. http://dx.doi.org/10.1590/S0104-77602012000300015

Nisgoski, S.; Magalhães, W.L.E.; Batista, F.R.R.; França, R.F.; Muñiz, G.I.B. de. 2014. Características anatômicas e energéticas do carvão de cinco espécies. *Acta Amazon* 44(3): 367-372. https://dx.doi.org/10.1590/1809-4392201304572

Nogueira, K.; Penatti, O.A.B.; dos Santos, J.A. 2017. Towards better exploiting convolutional neural networks for remote sensing scene classification. *Pattern Recogn* 61: 539-556. https://doi.org/10.1016/j.patcog.2016.07.001

Oliveira, J.T. 1997. Caracterização da madeira de eucalipto para a construção civil. Ph.D. Thesis, Univer-sidade de São Paulo, São Paulo, Brazil.

Paske, A.; Gross, S.; Massa, F.; Lerer, A.; Bradbury, J.; Chanan, G.; Killeen, T.; Lin, Z.; Gimelshein, N.; Antiga, L.; Desmaison, A.; Kopf, A.; Yang, E.; DeVito, Z.; Raison, M.; Tejani, A.; Chilamkurthy, S.; Steine, B.; Fan, L.; Bai, J.; Chintala, S. 2019. Pytorch: An imperative style, high-performance deep learning library. *Advances in neural information systems* 32 (2019). 8026-8037.

Pereira, B.L.C.; Oliveira, A.C.; Carvalho, A.M.M.L.; Carneiro, A. de C.O.; Santos, L.C.; Vital, B.R. 2012. Quality of wood and charcoal from eucalyptus clones for ironmaster use. *Int J For Res* Article ID 523025. https://doi.org/10.1155/2012/523025

Ponti, M.A.; Ribeiro, L.S.F.; Nazare, T.S.; Bui, T.; Collomosse, J. 2017. Everything you wanted to know about deep learning for computer vision but were afraid to ask. In 30th SIBGRAPI conference on graph-ics, patterns and images tutorials (SIBGRAPI-T). 17-41. Niterói, Brazil. https://doi.org/10.1109/SIBGRA-PI-T.2017.12

Rodrigues, L.F.; Naldi, M.C.; Mari, J.F. 2020. Comparing convolutional neural networks and pre-processing techniques for HEp-2 cell classification in immunofluorescence images. *Comput Biol Med* 116: 103542. https://doi.org/10.1016/j.compbiomed.2019.103542

Santos, R.C. 2010. Parâmetros de qualidade da madeira e do carvão vegetal de clones de eucalipto. Ph.D. Thesis, Universidade Federal de Lavras, Lavras, Brazil. http://repositorio.ufla.br/jspui/handle/1/2775

Scherer, D.; Müller, A.; Behnke, S. 2010. Evaluation of pooling operations in convolutional architectures for object recognition. In: International Conference on Artificial Neural Networks. Springer: Berlin, Heidel-berg. p. 92-101. https://doi.org/10.1007/978-3-642-15825-4_10

Simonyan, K.; Zisserman, A. 2014. Very deep convolutional networks for large-scale image recognition. arXiv preprint arXiv:1409.1556. https://arxiv.org/pdf/1409.1556.pdf

Szegedy, C.; Vanhoucke, V.; Ioffe, S.; Shlens, J.; Wojna, Z. 2016. Rethinking the inception architecture for computer vision. IEEE Conference on Computer Vision and Pattern Recognition (CVPR). 2818-2826, Las Vegas, NV, USA. https://ieeexplore.ieee.org/document/7780677

Tomazello-Filho, M. 1985. Estrutura anatômica da madeira de oito espécies de eucalipto cultivadas no Brasil. *IPEF* 29: 25-36, Brazil. https://www.ipef.br/publicacoes/scientia/nr29/cap03.pdf

Zenid, G. J.; Ceccantini, G.C. 2012. *Identificação macroscópica de madeiras*. *IPT*, São Paulo, Brazil.

Zhu, X.X.; Tuia, D.; Mou, L.; Xia, G.S.; Zhang, L.; Xu, F.; Fraundorfer, F. 2017. Deep learning in remote sensing: A comprehensive review and list of resources. *IEEE Geosc Rem Sens M* 5(4): 8-36. https://doi.org/10.1109/MGRS.2017.2762307

Wheeler, E.A.; Baas, P. 1998. Wood identification-a review. *Iawa J* 19(3): 241-264. https://doi.org/10.1163/22941932-90001528